Int. J. Heat Mass Transfer. Vol. 27, No. 10, pp. 1715–1723, 1984
Printed in Great Britain

0017–9310/84 $3.00 + 0.00

Effect of rounding of protruding edges on heat transfer and pressure drop in a duct

E. M. SPARROW and L. M. HOSSFELD
Department of Mechanical Engineering, University of Minnesota, Minneapolis, MN 55455, U.S.A.

(*Received* 14 *September* 1983 *and in revised form* 17 *November* 1983)

Abstract—Experiments were performed to determine the heat transfer, pressure drop, and flow field responses to the rounding of the peaks of a corrugated-wall duct. Two different degrees of corrugation-peak roundedness were used in addition to sharp (i.e. unrounded) corrugation peaks. The experiments encompassed the Reynolds number range from 2000 to 33 000 while the Prandtl number ranged from 4 to 11. It was found that at a given Reynolds number (i.e. given mass flow rate), the rounding of the corrugation peaks brought about a decrease in the Nusselt number which was accentuated at larger Reynolds numbers. The friction factor corresponding to a given Reynolds number decreased even more than did the Nusselt number. On the other hand, at equal pumping power, the Nusselt number was relatively insensitive to whether the peaks were sharp or rounded. Flow visualization experiments showed that rounding reduces the size of the separated region that is spawned at each corrugation peak.

INTRODUCTION

THERE are often significant deviations between the ideal geometries used in analysis or in conceptual design and those encountered in the passages of actual heat exchange devices. For example, depending on the method of fabrication, the successive peaks and valleys of the walls which bound a corrugated passage may be rounded rather than sharp. The fluid flow in a corrugated passage undergoes periodic changes of direction as it encounters the succession of peaks and valleys. However, for the velocities and corrugation angles of practical interest, the fluid is unable to follow the contour of the wall in the neighbourhood of the peaks and valleys so that flow separation occurs. It is likely that the nature of the separation will be affected by the sharpness (or roundedness) of the corrugations and, if so, the heat transfer and pressure drop characteristics of the channel will also be affected.

The foregoing discussion illustrating the effect of geometrical non-idealities on the fluid flow and heat transfer in a corrugated duct was motivated by the research to be reported here. In that research, the degree of roundedness of the corrugation peaks was varied systematically, and measurements were made of the response of the heat transfer coefficient and the pressure drop.

The corrugated duct is one member of a family of complex duct flows which are affected by the geometrical details of edges or tips over which fluid must pass. Another important member of this family is a pipe flow with ring-type inserts positioned periodically along the wall in order to disturb the laminar sublayer and enhance the heat transfer. Here, the nature of the flow disturbance and the degree of enhancement may be influenced by whether the edges of the rings are rounded or square. Rounded or square edges are also an issue in the case of periodically interrupted plate fins, especially when the fins are offset. As a final example, attention may be directed to the rounding of the edges of the air-cooled, block-like modules mounted on the circuit boards of electronic equipment.

Despite the potential importance of the edge-geometry issue with respect to heat transfer and pressure drop, it does not appear that systematic experiments involving both sharp- and rounded-edge versions of the same flow passage have been reported in the literature. Experiments of this type are described here for the corrugated duct. Two different degrees of corrugation-peak roundedness were used, and the corresponding heat transfer coefficients and friction factors are compared with those for the sharp-peak case. The comparisons are made both for equal Reynolds numbers for the compared ducts (i.e. equal mass flow rates) and for equal pumping power. Flow visualizations were also performed to examine the changes in the flow patterns adjacent to the duct walls in response to the rounding of the corrugation peaks.

The experiments were performed with water as the working fluid. Data were collected over the Reynolds number range from 2000 to 33 000. By varying the temperature level of the water, the Prandtl number was varied over the range from 4 to 11.

The heat transfer coefficients and friction factors for the duct with sharp-edged corrugations were taken from ref. [1], which is the forerunner of the present study and which dealt with issues such as the effects of interwall spacing, turning of the flow at the duct inlet, and leakage of heat into the duct sidewalls.

THE EXPERIMENTS

Heat transfer

A schematic diagram showing a representative portion of the sharp-edge version of the corrugated duct used in the heat transfer experiments is presented in Fig. 1. The duct configuration is characterized by the

NOMENCLATURE

A_{cyc}	convective heat transfer area per cycle
D_h	hydraulic diameter, $2HW/(H+W)$
f	fully developed friction factor, $(-dp/dx)D_h/\frac{1}{2}\rho V^2$
H	interwall spacing
h	cycle-average fully developed heat transfer coefficient, $Q_{cyc}/(T_w - T_b)_{fd}A_{cyc}$
k	thermal conductivity
$\dot{m}$	mass flow rate
Nu	cycle-average fully developed Nusselt number, hD_h/k
P	perimeter, $2(H+W)$
PP	pumping power
Pr	Prandtl number
p	pressure
Q_{cyc}	rate of heat transfer per cycle
Re	Reynolds number, $4\dot{m}/\mu P$
S	axial length of a cycle
T_b	bulk temperature
T_w	wall temperature
V	mean velocity
W	duct width
x	axial coordinate.

Greek symbols

θ	slope angle of facet
μ	viscosity
ρ	density.

Subscript

fd	fully developed.

interwall spacing H, the axial length S of a cycle in the periodic distribution of peaks and valleys, and the slope angle θ, the respective values of which are 0.737 cm, 2.032 cm, and 30°. In the direction normal to the plane of the figure, the duct had a width $W = 5.08$ cm, resulting in a cross-sectional aspect ratio $W/H = 6.9$. The entire duct encompassed ten corrugation cycles.

The duct consisted of the two corrugated walls shown in Fig. 1 (the principal walls) and a pair of sidewalls. All walls were made of copper. Heating was accomplished by an electric resistance wire embedded in grooves that had been machined in the rear face of each of the corrugated walls. There were 75 such transverse grooves in each wall, uniformly distributed along the length. Each principal wall was equipped with 20 thermocouples, with the respective junctions positioned within 0.025 cm of the inside wall of the duct. The thermocouples were installed so that their axial separation was $\frac{1}{2}S$. This installation was adopted to take advantage of the periodic character of the temperature field. Additional thermocouples were used to measure temperatures at selected sidewall locations.

The corrugated duct was incorporated into an open-loop, gravity-driven, water-flow facility. Special defenses against extraneous heat losses were built into the interfaces between the duct and the upstream and downstream plenum chambers which, respectively, fed water to the duct and received its discharge. Water was supplied to the system by an elevated constant-head tank connected to the hot and cold water building lines. By mixing the hot and cold water in any desired proportion, a preselected temperature level and

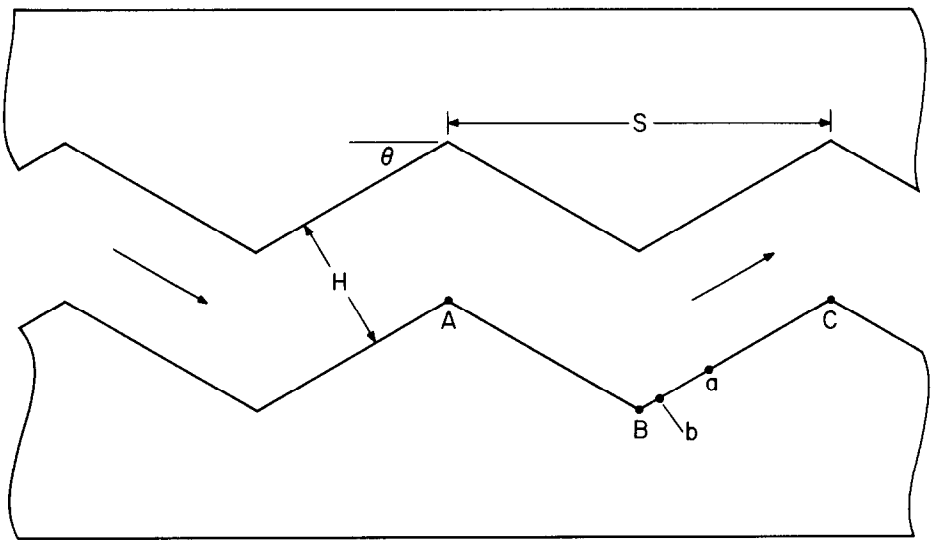

FIG. 1. Representative portion of the sharp-edge version of the corrugated duct used in the heat transfer experiments.

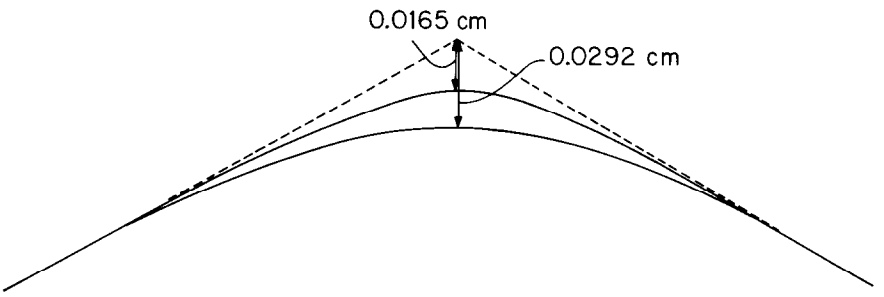

FIG. 2. Contours of the rounded and sharp corrugation peaks.

Prandtl number could be attained. The mass rate of water flow through the system was measured by the weight-tank method, with the water being collected at the exit of the downstream plenum.

For the study of the effect of corrugation-peak roundedness, modifications were made of the sharp-edge corrugated duct shown in Fig. 1. A special tool was ground and used in conjunction with a horizontal milling machine to round the initially sharp peaks of all the corrugations of both principal walls. Subsequent to these operations, the resulting contour of a representative peak was measured with a dial gage with a smallest scale division of 0.0001 in. The measured contour is reproduced in Fig. 2 as the uppermost solid line. Also shown as a dashed line is the original sharp-edged peak. As indicated there, the machining removed 0.0165 cm from the peak. Considering that the original peak-to-valley separation distance was 0.851 cm, it is evident that little change was made in the cross-section dimensions by the rounding of the peaks.

After the heat transfer data runs had been performed with the rounded-peak version of the corrugated duct, further rounding was created by milling with a second special tool. The outcome of the second machining operations is shown as the lower solid line in Fig. 2, where it is seen that the peak has been lowered by 0.0292 cm from its original height. Heat transfer experiments were then performed using the second rounded version of the corrugated duct.

It should be noted that no machining operations were performed to modify the valleys of the corrugations. Indeed, if the valleys were to be rounded to match the rounding of the peaks, material would have had to be added to the valleys, not removed. This was not deemed to be a feasible operation. Furthermore, evidence can be cited to support the view that it is immaterial whether or not the valleys are rounded.

In this regard, reference may be made to Fig. 1. From flow visualization studies reported in ref. [1], it was found that flow separation at a peak such as point A spawns a recirculation zone which not only blankets the rear-facing facet AB, but also blankets the portion Ba of the adjacent forward-facing facet BC. In particular, this recirculation zone blankets the valley bottom. As a consequence, the mainflow which passes through the duct is unaware of the true shape of the valley bottom. Therefore, the rounding or non-rounding of the valleys should have no material effect on the results.

Pressure drop and flow visualization

An apparatus separate from that for the heat transfer experiments was used for the pressure drop and the flow visualization studies. This second apparatus was made of Plexiglas (to facilitate the flow visualization), and the internal dimensions of the corrugated duct were made identical to those of the heat transfer duct by using the same tools to machine the corrugations of both ducts. Furthermore, in common with the heat transfer duct, two degrees of roundedness (those of Fig. 2) were successively machined into the Plexiglas duct.

A pressure tap was installed in each of the facets of one of the corrugated walls. Each tap was positioned at the spanwise and streamwise midpoint of its facet. Thus, every other facet is separated by the cycle length S which, as will be explained later, is a requisite for the proper interpretation of the pressure data.

Air was the working fluid in both the pressure drop and flow visualization experiments. The pressure measurement instrumentation for airflow is of greater accuracy and resolving power than that available for water flow. In the present experiments, a Baratron solid-state, capacitance-type meter was used to read the pressure signals.

The flow visualization was accomplished with the oil–lampblack technique. A mixture of oil and lampblack powder of appropriate fluidity was applied to the lower wall of the duct, whose facets had previously been covered with white, self-adhering, plasticized contact paper. The contact paper not only provided contrast but its removability from the duct wall after a visualization run enabled the traces of the flow pattern to be preserved and photographed.

To facilitate the visualization work, the upper wall of the Plexiglas duct was made removable. This feature enabled the easy application of the oil–lampblack mixture prior to the visualization run and the removal of the contact paper at the conclusion of the run. The development of the visualization pattern during the run was viewed by looking downward through the upper wall.

RESULTS AND DISCUSSION

The focus of this investigation is to determine the response of the fully developed Nusselt number and friction factor to rounding of the corrugation facets. The presentation of results will begin with the Nusselt numbers and then proceed to the friction factors. To supplement and illuminate these results, rounding-related changes in the pattern of fluid flow will be presented and discussed. The no-rounding and with-rounding results will then be compared both for equal mass flow rate and equal pumping power.

Nusselt number

As discussed in ref. [1], the thermally developed regime for a duct with a periodically varying flow, such as that being investigated here, is fundamentally different from that for a conventional, constant cross-section duct. For a uniformly heated periodic flow, a plot of the wall temperature as a function of the axial coordinate will not yield a straight line, neither in the thermally developing nor thermally developed regimes. However, in the developed regime, the wall temperatures at a succession of points separated from each other by an axial distance S (equal to the cycle length) lie on a straight line. Similarly, the fluid bulk temperatures at the same set of axial points lie on a straight line whose slope is equal to that of the aforementioned wall temperature line. The displacement of the two lines yields the fully developed wall-to-bulk temperature difference $(T_w - T_b)_{fd}$. Another feature of the periodic thermally developed regime is that the cycle-average heat transfer coefficient is the same for all cycles.

Here, cycle-average fully developed heat transfer coefficients will be evaluated from the experimental data via the defining equation

$$h = Q_{cyc}/(T_w - T_b)_{fd} A_{cyc} \tag{1}$$

where Q_{cyc} is the rate of heat transfer per cycle, and $(T_w - T_b)_{fd}$ is determined from plots of T_w and T_b as a function of the axial coordinate as discussed in the preceding paragraph. The quantity A_{cyc} represents the convective heat transfer area per cycle. There is some ambiguity inherent in the evaluation of the A_{cyc} because the duct sidewalls, while not directly heated, may receive heat by conduction from the principal walls and then transfer it to the fluid by convection. The issue of the sidewall participation was treated at length in ref. [1] and needs no further elaboration here.

Since the present interest is to obtain heat transfer coefficients for the rounded-peak cases relative to those for the sharp-peaked case, any procedure for evaluating A_{cyc} will be acceptable provided that it is used consistently. The simplest choice for A_{cyc} is the surface area of the principal walls per cycle, and that choice has been adopted here.

If the hydraulic diameter D_h is used as the characteristic dimension, the cycle-average Nusselt number follows as

$$Nu = hD_h/k \tag{2}$$

where $D_h = 2HW/(H+W)$. With the measured mass flow rate $\dot{m}$ of the water, the Reynolds number was evaluated from

$$Re = 4\dot{m}/\mu P, \quad P = 2(H+W). \tag{3}$$

The fluid properties which appear in equations (2) and (3) and in the Prandtl number Pr were evaluated at the mean bulk temperature. Property variations were a minor issue since the inlet-to-exit bulk temperature rises were limited to the order of 1°F.

A key ingredient in the presentation of the heat transfer results is the Nusselt numbers for the sharp-peaked case. This information is available from ref. [1] in the form of a least-squares fit of the experimental data. The fitted equation is a power law given by

$$Nu = 0.491\, Re^{0.632}\, Pr^{0.3}. \tag{4}$$

The Nusselt number results for the sharp- and rounded-peak corrugated ducts are presented in Fig. 3. The results for the sharp-peaked case are represented by a solid line which expresses equation (4). For the rounded-peak cases, the open symbols are for the lesser roundedness and the black symbols are for the greater roundedness. The data are also grouped according to Prandtl number, the nominal values of which are 4, 7, and 11. By plotting $Nu/Pr^{0.3}$ instead of Nu itself, the effect of Prandtl number has been eliminated from the data.

Examination of Fig. 3 shows that the rounding of the corrugation peaks brings about a decrease in the Nusselt number relative to the sharp-peaked case and that the decrease is accentuated with greater rounding. In the Reynolds number range between 2000 and 10 000, the with-rounding data are parallel to those for no rounding. For the two degrees of roundedness investigated here, the data respectively fall 3 and 8% below the non-rounded data.

For Reynolds numbers above 10 000, the deviations between the with-rounding and no-rounding Nusselt numbers tend to increase. Thus, at $Re = 30\,000$, the data for the lesser-rounded case lie about 11% below those for the non-rounded case, while for the more-rounded case the data are about 18% below the non-rounded data.

The rounding-related decreases in the Nusselt number evidenced in Fig. 3 are related to changes in the pattern of fluid flow due to rounding, with the changes in the size and structure of the separated region spawned by the peak being especially important. These factors will be discussed more fully when the flow visualization results are presented.

Another possible factor which might contribute to the Nusselt number decrease with rounding is the loss of heat transfer surface area which accompanies the rounding. In the present experiments, the facet surface area was decreased by only 0.65% due to the greater of the two investigated roundings. Thus, the area change was of no consequence.

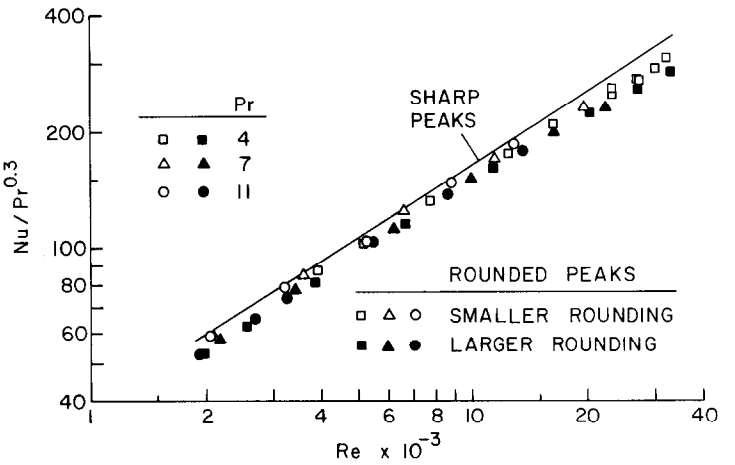

FIG. 3. Cycle-average fully developed Nusselt numbers for sharp- and rounded-peak corrugated ducts.

Friction factor

In the fully developed regime, the pressure exhibits periodicity characteristics similar to those already ascribed to the temperature. If the pressure were to be plotted as a function of the axial coordinate, the resulting distribution would not fall along a straight line. However, the pressures at successive points separated by the cycle length S do lie along a straight line. In the experimental apparatus, the pressure taps at the successive front-facing facets are separated by a distance S, and the measured pressures did, indeed, fall on a straight line. Similarly, the pressures measured at the successive rear-facing facets also fell on a straight line. In accordance with the properties of the periodic fully developed regime, the two lines were not coincident, but they were virtually identical in slope. The axial pressure gradient $-\mathrm{d}p/\mathrm{d}x$ was evaluated as the average of the two slopes.

With $-\mathrm{d}p/\mathrm{d}x$ as input, the friction factor was determined from its definition

$$f = (-\mathrm{d}p/\mathrm{d}x)D_h/\tfrac{1}{2}\rho V^2. \quad (5)$$

In this equation, $\rho V^2 = (\dot{m}/HW)^2/\rho$, where ρ is the mean density in the fully developed regime.

The friction factors for the sharp- and rounded-peak ducts are listed in Table 1 as a function of the Reynolds number (the no-rounding data are from ref. [1]). From the table, it is seen that the friction factor is diminished by the rounding and that the more the rounding, the greater the decrease. This behavior complements the decrease in the Nusselt number with rounding that was encountered in the previous section. The percentage decreases in the friction factor are greater than those already identified for the Nusselt number. If the numerical values in each column of Table 1 are averaged over the Reynolds number, it is seen that the f's for the ducts with the smaller and larger roundedness are, respectively, 81 and 60% of the f for the non-rounded case.

Table 1. Fully developed friction factors for sharp- and rounded-peak ducts

Re	No rounding	Smaller rounding	Larger rounding
1950	1.22	1.07	0.831
3500	1.26	1.05	0.805
6300	1.35	1.06	0.782
11 000	1.36	1.07	0.760
18 500	1.37	1.06	0.742

Although the aforementioned rounding-related reductions in the friction factor appear attractive, account must also be taken of the accompanying Nusselt number reductions. These issues will be addressed in a later section.

Further inspection of Table 1 reveals that there is a slight dependence of f on Re and that the direction of this dependence is affected by the rounding of the peaks. For the no-rounding case, f increases with Re in the range of low Re and is more or less constant thereafter. The f values for the smaller of the two roundings are virtually independent of Re, while those for the larger rounding decrease with Re.

These changes in the shape of the f, Re distributions, taken together with the aforementioned changes in the level of f, suggest a rounding-related shift in the relative importance of the skin friction and inertial pressure losses. With greater rounding, the inertial losses decrease, thereby giving more weight to the skin friction losses. Since the inertial losses occur primarily in the separated region that is spawned at a corrugation peak, it may be conjectured that the size and/or the vigor of the separated region diminishes as the peaks are rounded. This conjecture will now be examined with the aid of the flow visualization results.

Flow visualization results

As noted earlier, the contact paper which covered the lower-wall corrugations during a flow visualization run was detached after the run and laid flat for photography. A pair of photographs which display

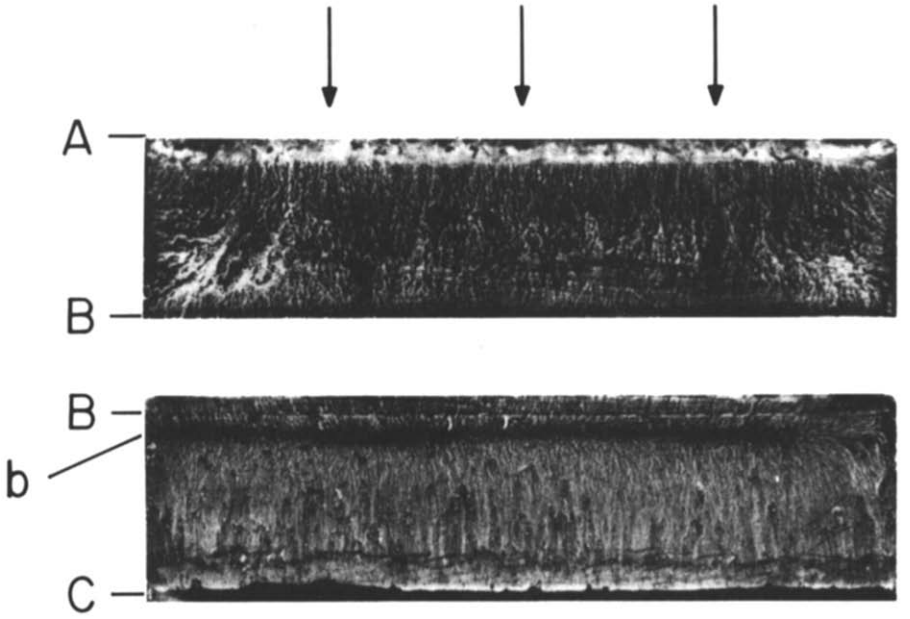

FIG. 4. Flow visualization patterns.

typical results of the visualization studies is shown in Fig. 4. These photographs, which are views looking down at the corrugation facets of the lower wall, correspond to a Reynolds number of approximately 30 000 and to the duct with the larger rounding of the corrugation peaks.

To facilitate the explanation of the photographs, it is useful to refer to Fig. 1. There, a typical rear-facing facet has been designated as AB, while the forward-facing facet immediately downstream of AB is designated as BC. These same designations are used to identify the respective photographs of Fig. 4. The upper photograph corresponds to a rear-facing facet, and the letters A and B have been affixed to identify the peak and the valley. The lower photograph is for the adjacent forward-facing facet downstream of AB, and the valley and the peak are respectively identified by letters B and C. Vectors situated along the upper edge of the figure depict the direction of the mainflow.

Prior to the initiation of the airflow during a visualization run, the oil–lampblack mixture that had been applied to the contact paper appeared uniformly black to the eye. Thus, the streaks and bands which can be seen in the photograph were created by the air movement adjacent to the facets.

Attention may first be turned to the photograph of the forward-facing facet BC. The most significant landmark that can be seen in this photograph is the dark horizontal band identified by the letter b. This is the line which marks the downstream closure of the separated region which was spawned by the peak A; that is, the mainflow which separates from the duct wall at A reattaches to the wall at b. The location of the reattachment line b is also shown in Fig. 1.

In the region bC on the forward-facing facet BC, the wall-adjacent flow is in the direction from b to C, which is the mainflow direction. Finely etched streaks in the region bC (Fig. 4) provide evidence of this wall-adjacent flow. On the other hand, in the region Bb, the wall-adjacent flow is a backflow, that is, the fluid moves in the direction from b to B.

The backflow blankets the entirety of the rear-facing facet AB (i.e. the flow moves along the surface from B to A). The backflow is the wall-adjacent leg of a recirculating flow which fills the separated region. In the photograph (Fig. 4), the streaklines are the tracks of the backflow. These lines reflect the presence of three-dimensional motions adjacent to the sidewalls of the duct (left- and right-hand edges of the photograph), and these motions appear especially pronounced in the neighborhood of the valley (left- and right-hand corners).

The white band appearing just below the upper edge of the upper photograph and the fine black band appearing somewhat above the lower edge of the lower photograph are imperfections that are unrelated to the fluid flow processes being studied. The white band resulted when an accumulation of the oil–lampblack mixture, driven 'uphill' along the facet AB by the backflow, was soaked up with an absorptive tissue (to avoid sagging when the airflow was terminated). On the other hand, the fine black band is due either to a partial soaking up of the mixture or to nonuniform initial application of the mixture.

Figure 4 corresponds to the highest Reynolds number of the experiments. In general, it was found that definitive visualization patterns were obtainable only at high Reynolds numbers. As a consequence, changes in the flow pattern with Reynolds number could not be identified.

It is relevant to compare the visualization pattern for the rounded-peak case, as conveyed by Fig. 4, to that for

the non-rounded case which is shown in Fig. 3 of ref. [1]. The most significant difference between the two patterns is in the size of the separated region spawned at a corrugation peak. This difference is illustrated with the aid of Fig. 1. For separation spawned at a sharp peak A, reattachment occurs at point a. On the other hand, if peak A is rounded (i.e. the greater of the two roundings), point b is the reattachment point.

Thus, rounding of the peaks diminishes the size of the separated region. As a consequence, the inertial losses are reduced and the skin friction losses gain in relative importance, so that the reduction of the friction factor with rounding and the tendency for f to decrease with Re are plausible.

Rounding not only reduces the size of the disturbed region but also tends to diminish the general disturbance level. These factors are believed to be responsible for the reduction in the heat transfer coefficient with rounding.

PERFORMANCE EVALUATIONS

It remains to inquire about the relative performance of sharp-peak vs rounded-peak ducts. This issue has to be dealt with in a manner similar to that used for the performance ranking of enhanced and unenhanced heat exchange devices. For such rankings to be meaningful, it is necessary to specify the constraints under which the comparison is being made (e.g. equal fluid flow rate, equal pumping power, equal pressure drop) and also to specify the quantity on which the ranking is based (e.g. heat transfer rate, heat transfer coefficient, pressure drop). In this paper, basic heat transfer and pressure drop data have been provided for both sharp- and rounded-peak ducts, so that performance evaluations can be made for whatever constraints and ranking parameters are appropriate to each specific application.

Here, only representative performance evaluations will be carried out. Two cases will be considered. In one, the sharp- and rounded-peak ducts are compared under the condition of equal fluid flow rate, while in the second, the comparison is made for equal pumping power.

Since the ducts being compared have virtually identical dimensions, it follows from equation (3) that the equal fluid flow rate condition is equivalent to the condition of equal Reynolds number. Consequently, Fig. 3 and Table 1 can be used directly to rank order the heat transfer and pressure drop performance of the sharp- and rounded-peak ducts. If the rank is ordered according to the largest heat transfer rate (or heat transfer coefficient), then the sharp-peak duct is best. However, if the ranking is made according to the least pressure drop, then the duct with the more-rounded peaks is best.

In contrast to the equal flow rate constraint, where the heat transfer and pressure drop characteristics are considered separately, the equal pumping power constraint brings these characteristics together. The pumping power PP can be expressed as

$$PP = (\dot{m}/\rho)\Delta p. \tag{6}$$

For two ducts i and j, the condition of equal pumping power is satisfied when

$$(f\,Re^3)_i = (f\,Re^3)_j \tag{7}$$

or

$$Re_i = (f_j/f_i)^{1/3}\,Re_j. \tag{8}$$

By using the friction factors listed in Table 1, the Reynolds numbers corresponding to equal pumping power for the three investigated ducts have been calculated and are presented in Table 2 (first, third, and fifth columns). In Table 2, each line corresponds to a given pumping power. As expected, at equal pumping power, the rounded-peak ducts can be operated at higher Reynolds numbers than that for the sharp-peak duct.

The equal-pumping-power Reynolds numbers of Table 2 were used to read Nusselt numbers from Fig. 3. These equal-pumping-power Nusselt numbers are listed in the second, fourth, and sixth columns of Table 2. The table shows that over most of the investigated Reynolds number range, the equal-pumping-power Nusselt numbers for the three ducts are virtually identical. Only at the higher Reynolds numbers is there a 5–6% spread, with the sharp-peak duct providing the highest Nusselt number values. Thus, on the basis of equal pumping power, rounding of the corrugation peaks has little effect on the heat transfer coefficients.

Table 2. Equal-pumping-power Reynolds and Nusselt numbers

No rounding		Smaller rounding		Larger rounding	
Re	$Nu/Pr^{0.3}$	Re	$Nu/Pr^{0.3}$	Re	$Nu/Pr^{0.3}$
2000	59.9	2100	60	2300	59.6
3000	77.4	3160	77.5	3500	77.5
5000	106.9	5300	107	5900	108
8000	143.8	8700	146	9700	147
11 000	175.9	11 960	176	13 400	176
15 000	214.0	16 310	210	18 300	209
20 000	256.6	21 750	246	24 400	244
25 000	295.5	27 200	279	30 800	277

CONCLUDING REMARKS

The work reported here is, seemingly, the first systematic experimental study of the effect of rounding of protruding or exposed edges on forced convection heat transfer and pressure drop in ducts. The experiments were performed with a corrugated duct which had initially been fabricated with sharp peaks and valleys. Subsequently, the peaks were slightly rounded, and heat transfer and pressure drop data were collected. Then, the peaks were additionally rounded, and further data were collected.

With water as the working fluid, the heat transfer experiments were carried out over the Reynolds number range from 2000 to 33 000 and for Prandtl numbers between 4 and 11. To supplement the heat transfer and pressure drop measurements, flow visualizations were performed to reveal the rounding-related changes in the patterns of fluid flow adjacent to the duct walls. Both the pressure drop and visualization experiments were carried out in an airflow apparatus. To quantify the roundedness of the peaks, surface contour measurements were made and are reported in the paper.

Cycle-average fully developed Nusselt numbers were evaluated for the ducts with the two different degrees of corrugation peak roundedness, and these results were compared with corresponding results for the sharp-peak corrugated duct. At a fixed Reynolds number, rounding of the corrugation peaks brought about a decrease in the Nusselt number, and the extent of the decrease was accentuated with greater rounding. In the lower portion of the investigated Reynolds number range ($2000 \leqslant Re \leqslant 10\,000$), the rounding-related reductions were moderate—no more than 8%. At higher Reynolds numbers, larger reductions, up to 18% at $Re = 30\,000$, occurred. The rounding of the peaks also brought about a decrease in the fully developed friction factor at a fixed Reynolds number. For the duct with the more-rounded corrugations, the friction factors were about 60% of those for the sharp-peak corrugations.

The flow visualization experiments showed that rounding reduces the size of the separated region that is spawned at each corrugation peak. The associated reduction in the inertial-type pressure losses is mainly responsible for the smaller friction factor values for the rounded-peak ducts. Rounding not only reduces the size of the separated region but also tends to diminish the general disturbance level of the flow, which brings about the observed reduction in the heat transfer coefficient.

The foregoing fixed-Reynolds-number comparison of results for the sharp- and rounded-peak ducts is equivalent to comparing at a fixed fluid flow rate. The results were also compared on the basis of equal pumping power. For that constraint, the Nusselt number was found to be insensitive to rounding of the corrugation peaks except in the upper range of the investigated Reynolds numbers, where rounding was responsible for a 5–6% decrease.

REFERENCE

1. E. M. Sparrow and J. W. Comb, Effect of interwall spacing and fluid flow inlet conditions on a corrugated-wall heat exchanger, *Int. J. Heat Mass Transfer* **26**, 993–1005 (1983).

EFFET DE LA COURBURE DES EXCROISSANCES SUR LE TRANSFERT THERMIQUE ET LA CHUTE DE PRESSION DANS UNE CONDUITE

Résumé—Des expériences sont faites pour déterminer l'influence sur le transfert thermique, la chute de pression et les champs de vitesse, de la courbure des pointes sur la paroi corruguée d'une conduite. Deux différents degrés d'arrondi des excroissances sont traités en supplément des pointes non arrondies. Les expériences couvrent le domaine 2000–33 000 pour le nombre de Reynolds, tandis que le nombre de Prandtl varie entre 4 et 11. On trouve qu'à un nombre de Reynolds donné (ou d'un débit donné), la courbure des extrémités conduit à une diminution du nombre de Nusselt laquelle est accentuée aux grands nombres de Reynolds. Le coefficient de frottement associé à un nombre de Reynolds constant décroît plus que ne le fait le nombre de Nusselt. D'autre part, à puissance égale de pompage, le nombre de Nusselt est relativement insensible au fait que les pointes sont aiguës ou non. Des expériences de visualisation montrent que l'arrondi réduit la taille de la région de séparation qui est engendré par la corrugation.

DER EINFLUSS DES ABRUNDENS VON VORSPRINGENDEN ECKEN AUF DEN WÄRMEÜBERGANG UND DRUCKABFALL IN EINEM KANAL

Zusammenfassung—Versuche wurden durchgeführt, um das Verhalten von Wärmeübergang, Druckabfall und Strömung als Folge des Abrundens der Spitzen der geriffelten Wände eines Kanals zu untersuchen. Zwei verschiedene Abrundungsgrade der Spitzen wurden außer den scharfen (d. h. ungerundeten) Spitzen berücksichtigt. Bei den Versuchen lag die Reynolds-Zahl im Bereich zwischen 2000 und 33 000, die Prandtl-Zahl zwischen 4 und 11. Es zeigte sich, daß bei einer gegebenen Reynolds-Zahl (d. h. gegebenem Massenstrom) die Abrundung der Spitzen eine Abnahme der Nusselt-Zahl bewirkt, und zwar um so mehr, je höher die Reynolds-Zahl war. Der zu einer bestimmten Reynolds-Zahl gehörende Reibungsbeiwert nahm dabei stärker ab als die Nusselt-Zahl. Andererseits war die Nusselt-Zahl bei gleicher Pumpleistung relativ unempfindlich dagegen, ob die Spitzen scharf oder abgerundet waren. Versuche mit Strömungssichtbarmachung zeigten, daß durch die Abrundung die Länge des von jeder Riffelspitze ausgehenden Ablösungsgebiets verringert wird.

ВЛИЯНИЕ СКРУГЛЕНИЯ ОСТРЫХ ВЫСТУПОВ ШЕРОХОВАТОСТИ НА ТЕПЛОПЕРЕНОС И ПАДЕНИЕ ДАВЛЕНИЯ В КАНАЛЕ

Аннотация—Проведено экспериментальное исследование влияния скругления острых выступов рифленых стенок канала на перенос тепла, падение давления и поле течения. Исследовались каналы с двумя различными степенями скругления и канал с острыми (т.е. нескругленными) выступами шероховатости. Эксперименты проводились в диапазонах значений числа Рейнольдса от 2000 до 33 000 и числа Прандтля от 4 до 11. Найдено, что при заданном значении числа Рейнольдса (т.е. при заданной интенсивности массопереноса) скругление острых выступов шероховатости приводило к снижению числа Нуссельта, причем более заметному при больших значениях числа Рейнольдса. Величина коэффициента трения, соответствующая заданному значению числа Рейнольдса, уменьшалась гораздо больше, чем число Нуссельта. С другой стороны, при одной и той же мощности подачи жидкости число Нуссельта относительно не зависело от степени заостренности выступов. Эксперименты по визуализации потока показали, что скругление выступов уменьшает размеры отрывных областей, образующихся вблизи выступов шероховатости.